

# Effect of temperature on the structure and dynamic properties of metal sulphide nanostructures via molecular dynamics simulation

**M A Mehlape, T G Mametja, T E Letsoalo and P E Ngoepe**

Materials Modelling Centre, School of Physical and Mineral Sciences, University of Limpopo, South Africa, Private Bag, X1106, SOVENGA, 0727

Email:mofuti.mehlape@ul.ac.za

**Abstract.** Metal sulphide nanostructures via molecular dynamics (MD) simulations at different temperatures are presented and discussed in order to understand their structure and dynamic properties. Nanostructured metal sulphides have attracted the attention of researchers in the fields of materials science, physics and chemistry. They have enhanced structure and dynamic properties due to their large surface-to-volume ratio; hence making them desirable to a wide range of industries. They are promising materials for catalysis, batteries and photovoltaic, however the understanding on the structure and dynamic conditions of large-scale nanostructures are still to be explored more. Computational modelling technique, MD was performed to provide atomic or molecular level insights of the structure and dynamic properties of nanostructured metal sulphides. The effect of temperature on different sizes of nanostructures are analysed in a form of structure and dynamic properties; namely radial distribution functions, potential energy and diffusion coefficient. The results showed that temperature associated with the melting transition and stability increased with an increase in the nanostructure size. New insight into MD study of nanostructured metal sulphides is obtained and providing guidance to experiments.

## 1. Introduction

Nanoscience and nanotechnology collectively represent one of the fastest growing interdisciplinary scientific areas, spanning interests from physics, through chemistry and geoscience, to biology [1]. Nanostructures have been identified worldwide as the key to unlocking a new generation of devices with revolutionary properties and functionalities [2]. Nanostructures have many interesting properties (for example structural and dynamic properties), as they bridge the gap between bulk materials and atomic or molecular structures [3]. Nanostructures offer the advantages of high surface-to-volume ratios, favourable transport properties, and high freedom for the volume change [4]. Herein, we report the effect of temperature on the structure and dynamic properties of metal sulphide, FeS<sub>2</sub> pyrite nanostructures. Pyrite, also known as Fool's Gold, is a very attractive next-generation photovoltaic (PV) material that is abundant in nature and nontoxic [5]. Various FeS<sub>2</sub> pyrite nanostructures such as nanostructures [6], nanocrystals [7], nanotubes [8] and nanowires [9] to name but a few, have been studied experimentally. However, experimental difficulties in studying nanostructures arise from their small size, which limits the use of traditional techniques for measuring other properties and conditions (such as physical, structural and dynamic properties, pressure and temperature) [10]. Hence, computational simulation is used to access those conditions that are sometimes difficult to obtain experimentally and simulation is also useful for planning experiments that require complicated setups

[11]. Computational simulation technique, molecular dynamics (MD) is used to investigate the effect of temperature on the structure and dynamic properties of FeS<sub>2</sub> nanostructures.

### 1.1. Pyrite, FeS<sub>2</sub> structure

Cubic pyrite, FeS<sub>2</sub> belongs to the space group Pa3 [12]. FeS<sub>2</sub> has a NaCl-type cubic structure with the (S<sub>2</sub>)<sup>2-</sup> groups situated at the cube centre and midpoints of the cube edges, and the low-spin Fe<sup>2+</sup> atoms located at the corners and face centres [13]. Cubic FeS<sub>2</sub> structure together with the nanostructure are shown in Figure 1.

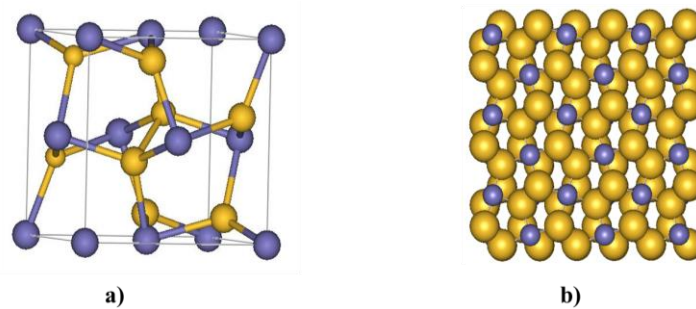


**Figure 1:** Snapshots of a) cubic bulk structure of pyrite, FeS<sub>2</sub>, and b) Initial FeS<sub>2</sub> nanostructure, where purple atoms represent iron (Fe) and yellow atoms represent sulphur (S).

## 2. Computational Details

### 2.1. Creation of nanostructures and methodology

Initial configuration of FeS<sub>2</sub> nanostructures was constructed using METADISE code [14], which uses Wulff constructions [15] to predict the morphology. This approach follows the theory of Gibbs to generate the lowest total surface energy morphology from facets that may each have different surface energies. The stable {100} surface [16] was used to create its cubic nanostructures.

MD simulations of nanostructures were performed with DLPOLY\_2.20 code [17]. The MD simulation of the nanostructures were carried out in an ensemble approximating the canonical with constant number of atoms N and volume V. Temperature is controlled by a Nose-Hoover thermostat [18] and the equation of motion were integrated using the Verlet Leapfrog algorithm [19] with a time step of 1 fs. The constant temperature and volume simulations were performed over the temperature range of 300 K to 2000 K with 100 K increments at zero pressure for the NPs of between 1 nm and 4.5 nm in diameter. The sizes of the nanostructures of FeS<sub>2</sub> used in this study, and the corresponding number of FeS<sub>2</sub> units are given in Table 1. MD simulations were performed under non-periodic boundary conditions to make sure that the results are not affected by boundary conditions.

**Table 1:** Size of nanostructures (in diameter) and the corresponding number of FeS<sub>2</sub> units used for nanostructures.

Particle Dimension (nm)	Number of Atoms
1.0	96
1.5	324
2.9	1997
3.4	3295
4.5	7369

### 2.2. Representation of interatomic potentials

The Born ionic model [20] was used and parameters were derived for short range interactions represented by the Buckingham potential, harmonic function and three body terms:

#### 2.2.1. Buckingham Potential

In the Buckingham potential, the repulsive term is replaced by an exponential term and potential takes the form

$$U(r_{ij}) = A_{ij} * \exp^{-r_{ij}/\rho_{ij}} - \frac{C_{ij}}{r_{ij}^6} \quad (1)$$

where  $A_{ij}$  and  $\rho_{ij}$  are parameters that represent the ion size and hardness, respectively, while  $C_{ij}$  describe the attractive interaction and  $r_{ij}$  is the distance between ion  $i$  and ion  $j$ . The first term is known as the Born-Mayer potential and the attraction term (second term) was later added to form the Buckingham potential. Very often, for the cation-anion interactions, the attractive term is ignored due to the very small contribution of this term to the short-range potential, or, alternatively, the interaction is subsumed into the  $A$  and  $\rho$  parameters.

### 2.2.2. Harmonic Potential

The interaction between the sulphur atoms of the S-S pair were described by a simple bond harmonic function:

$$U(r_{ij}) = \frac{1}{2} k_{ij} (r_{ij} - r_0)^2 \quad (2)$$

where  $k_{ij}$  is the bond force constant,  $r_{ij}$  the interionic separation and  $r_0$  the separation at equilibrium.

### 2.2.3. Three-Body Potential

A further component of the interactions of covalent species is the bond-bending term, which is added to take into account the energy penalty for deviations from the equilibrium value. Hence, this potential describes the directionality of the bonds and has a simple harmonic form:

$$U(\theta_{ijk}) = \frac{1}{2} k_{ijk} (\theta_{ijk} - \theta_0)^2 \quad (3)$$

where  $k_{ijk}$  is the three-body force constant,  $\theta_0$  is equilibrium angle and  $\theta_{ijk}$  is the angle between two interatomic vectors  $i-j$  and  $i-k$ . The interatomic potentials used for this study were previously developed and modified for the simulation of bulk and surfaces of FeS<sub>2</sub> [16, 21].

## 3. Results and Discussions

### 3.1. Dynamic properties

Thermodynamically, the melting of bulk crystalline solids is characterized by a sudden increase in the free energy [22]. The curves of potential energy versus temperature for FeS<sub>2</sub> nanostructures were obtained. Figure 2 shows the potential energy variation with temperature for nanostructures with different number of atoms, i.e., 96, 324, 1997, 3295 and 7369 atoms, which corresponds to 1 nm, 1.5 nm, 2.9 nm, 3.4 nm and 4.5 nm in diameter, respectively. The phase transition from solid to liquid phase can be identified by a jump in the energy curve. The melting point of the FeS<sub>2</sub> nanostructures can be estimated from the change in slope of the temperature dependence of the energy. It can be noted that there is a change of slope at a certain temperature for different sizes of nanostructures. For the nanostructure with 96 atoms, although not clear an abrupt energy change occurs at a temperature of about 800 K. In the case of a nanostructure with 324 atoms, the change, even though it is not clear, is observed between the 800 K and 1000 K. For a nanostructure with 1997 atoms, the change is between 900 K and 1000 K and for nanostructure with 3295 atoms; the change of energy is noticed between 1000 K and 1100 K. For the nanostructure with 7369 atoms the energy variations with temperature is noticed between 1200 K and 1300 K. The rate of change of energy with increasing temperature for nanostructures with diameter of 1 nm, 1.5 nm, 2.9 nm and 3.4 nm is not the same as the one on 4.5 nm nanostructures. In case of the nanostructure of 4.5 nm there is a distinct increase in energy, whereby in the case of the other nanostructures the increase is not distinct. This implies that as the size of the nanostructure increase,

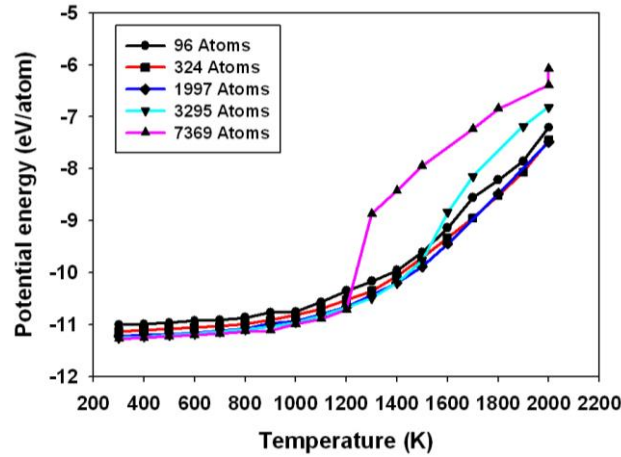


**Figure 2:** The potential energy per atom as a function of temperature for nanostructures with different number of atoms. Number of atoms corresponds to the diameters depicted on Table 1.

### 3.2. Structural properties

Typical RDF plots for FeS<sub>2</sub> nanostructures of 324 and 7369 atoms for Fe–Fe, Fe–S and S–S pairs at temperatures between 300 and 1500 K are shown in Figure 3. For the aim of determining the effect of temperature on Fe–Fe, Fe–S and S–S pairs of FeS<sub>2</sub> nanostructures. The RDF's change from well-ordered to molten configuration for increasing temperature. The well-ordered configuration is characterised by a profile which manifests a greater number of narrower peaks with increasing radius. The molten configuration is characterised by a profile with both fewer and broader peaks. It can be observed that the RDFs show structural changes at different temperatures for different sizes of nanostructures. The nanostructure with 324 atoms, in Figure 3(a), has a well-defined structure, as observed by many peaks of the RDFs, from 300 to 500 K. The height of the peaks is also reduced as the temperature increases. The significant peak height reduction for the Fe–Fe, Fe–S and S–S pairs is observed at 1000 K; in particular the peaks almost collapse, suggestive of the liquid phase of the nanostructure with 324 atoms. The nanostructures with 7369 atoms at the temperatures leading to the melting are shown in Figure 3(b). It can be deduced from the many peaks of the RDFs that from 300 to 1000 K, the nanostructures have a well-defined structure. At 1000 K the peaks start to broaden and the height of the peaks has decreased substantially as compared to those at lower temperatures; however at 1500 K the peaks beyond the first have almost disappeared, indicative of the liquid phase of the nanostructure with 7369 atoms.

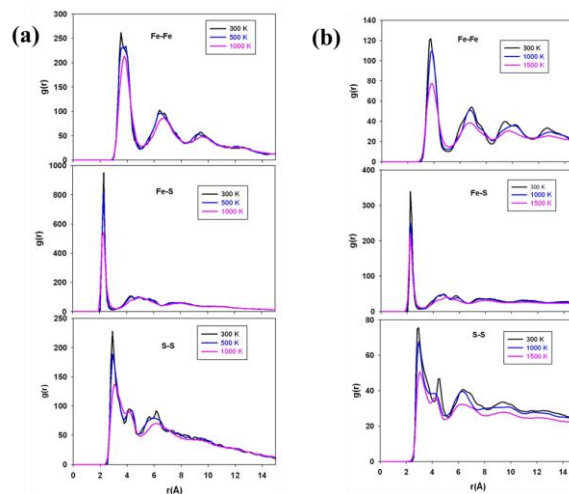


**Figure 3:** The radial distribution functions (RDFs) of FeS<sub>2</sub> nanostructures at various temperatures with different number of atoms. (a) 324 atoms and (b) 7369 atoms.

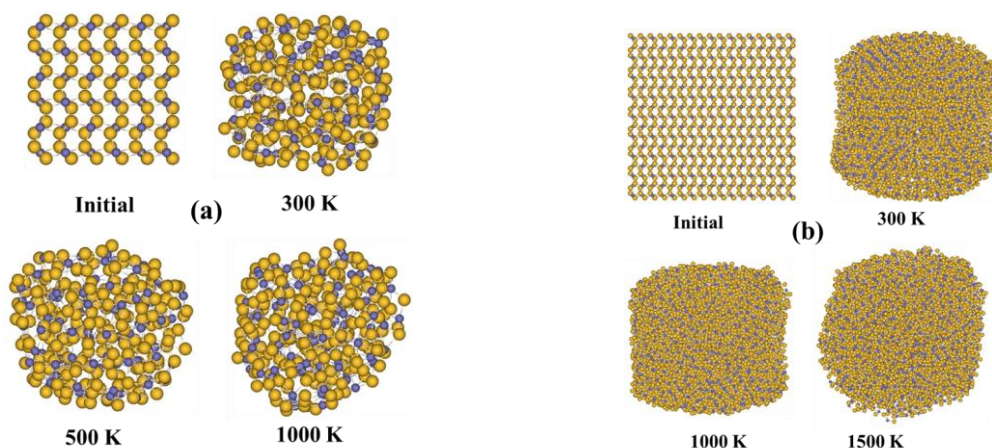


**Figure 4:** Structural changes of FeS<sub>2</sub> nanostructures with a) 324 atoms and b) 7369 atoms before and after MD simulation at different temperatures.

The initial configuration structures and structures after MD simulations at different temperatures of FeS<sub>2</sub> nanostructures are shown in Figure 4. It can be seen that the nanoparticles assume well-ordered cubic shapes at the initial configuration, and as the temperature is increased the atom packing is disordered. For a nanostructure with 324 atoms the cubic structure is maintained at the temperature of 300 K, however at the elevated temperatures (from 500 K), the atomic arrangement disappears. Meanwhile, with the nanostructure with 7369 atoms the cubic structure is maintained up to a temperature of 1000 K and the arrangement of atoms vanishes at a higher temperature of 1500 K. This implies that the stability of the nanostructure increases as the particle size increases.

#### 4. Conclusion

Molecular dynamics simulations were performed with the aim of investigating the dynamic and structural properties of pyrite FeS<sub>2</sub> nanostructures. It was observed that the temperature of melting transition increased with an increase in particle size. The melting of nanostructures was observed through the variation of energy as a function of temperature, whereby there is a sudden change of slope at a certain temperature, indicative of phase transition. The RDFs suggest that low temperatures have many and sharp peaks, at higher temperatures the peaks are few and smooth, which is indicative of phase transition. The height of the peaks is also reduced as the temperature increases. The structural snapshots suggest that the nanostructures with fewer number of atoms maintain their cubic structure up to 500 K and for the nanostructures with large number of atoms maintain their cubic form up to 1000 K. This implies that the stability of the nanostructure increases as the particle size increases. The results suggest that molecular dynamics understanding of FeS<sub>2</sub> nanostructures can serve to explain or predict their structural and dynamic properties, providing a guideline to experiments.

#### Acknowledgements

The computations were performed at the Materials Modelling Centre (MMC), University of Limpopo and at the Centre for High Performance Computing (CHPC), Cape Town. We also acknowledge the National Research Foundation (NRF) for funding.

#### References

- [1] Spagnoli D and Gale J G 2012 *Nanoscale* **4** 1051.
- [2] Akbarzadeh H, Abroshan H and Parsafar G A, 2010 *Solid State Commun.* **150**, 254.
- [3] Heikkilä E, Martínez-Seara A A, Hakkinen H, Vattulainen I and Akola J 2012 *J. Phys. Chem.* **166**, 9805.
- [4] Rui X, Tan H and Yan Q 2014 *Nanoscale* **6** 9889.

- [5] Bi Y, Exstrom C L, Darveau S A, Huang I, 2012 *Nano Lett.* **11**, 4953.
- [6] Chin P P, Ding J, Yi J B and Liu B H 2005 *J. Alloys. Compd.* **390** 255.
- [7] Trinh T K, Pham V T H, Truong N T N, Kim C D and Park C 2017 *J. Cryst. Growth.* **461** 53.
- [8] Macpherson H and Stoldt C R 2012 *ACS Nano* **6**, 8940.
- [9] Caban-Acevedo M, Faber M S., Tan Y, Hamers R J and Jin S 2012 *Nano Lett.* **12** 1977.
- [10] Suh Y J, Prikhodko S V, Friedlander S K *Microsc. Microanal.* 2002 **8** 497.
- [11] Rodrigues A M, Rino J P, Pizani P S and Zanotto E D 2016 *J. Phys. D: Appl. Phys.* **49** 1.
- [12] Liu S, Li Y, Yang J, Tian H, Zhu B and Shi Y 2014 *Phys. Chem. Miner.* **41** 189.
- [13] Huang S-Y, Sodano D, Leonard T, Luiso S and Fedkiw P S 2017 *J. Electrochem. Soc.* **164** F276.
- [14] Watson G W, Kelsey E T, de Leeuw N H, Harris D J and Parker S C 1996 *J. Chem. Soc. Faraday Trans* **92** 433.
- [15] Wulff G Z 1901 *Krystallogr. Minera.* **34** 449.
- [16] Mehlape M A, Parker S C and Ngoepe P E 2015 in *Proceedings of the 60th Annual Conference of the South African Institute of Physics* edited by M. Chithambo and A. Venter, (SAIP2015, Richard's Bay, South Africa,) 67.
- [17] Smith W and Forester T R 1996 *J. Mol. Graphics* **14** 136.
- [18] Nosé S 1990 *J. Phys.:Condens. Matter.* **2** 115.
- [19] Verlet L 1967 *Phys. Rev.* **159**, 98.
- [20] Born M and Huang K 1954 *Dynamical Theory of Crystal Lattices*, 1st ed. (University Press, Oxford).
- [21] de Leeuw N H, Parker S C, Sithole H M and Ngoepe P E 2000 *J. Phys. Chem. B* **104** 7969.
- [22] Adnan A and Sun C T 2008 *Nanotechnology* **19** 1.